ChemComm

COMMUNICATION

View Article Online
View Journal | View Issue

Cite this: *Chem. Commun.*, 2017, 53, 5645

Received 30th March 2017,
Accepted 2nd May 2017

DOI: 10.1039/c7cc02470c

rsc.li/chemcomm

Confinement effects of a crystalline sponge on ferrocene and ferrocene carboxaldehyde†

Gabriel Brunet,[a] Damir A. Safin,[ab] Koen Robeyns,[b] Glenn A. Facey,[a] Ilia Korobkov,[a] Yaroslav Filinchuk[b] and Muralee Murugesu*[a]

The pivotal role of π···π interactions in the inclusion behaviour of a series of organometallic sandwich compounds is studied through single-crystal X-ray diffraction. The confinement effects of a crystalline sponge host are investigated where, notably, we observe an enhanced rotation of the ligand ring once encapsulated by the nanoporous framework, as evidenced by SSNMR experiments.

Over the past two decades, the scientific community has witnessed the unprecedented development of a new class of crystalline materials capable of offering easily tuneable porous structures. These multi-functional materials, termed metal–organic frameworks (MOFs), have excelled in providing promising alternatives for select applications in gas separation,[1] catalysis,[2] drug delivery,[3] and chemical separation.[4] A common denominator among all such space-specific functions involves molecular adsorption of the desired guest. While multiple experimental methods can be used to confirm successful guest inclusion,[5] the direct visualization of host–guest interactions, which drive the uptake process, remains a challenge. This is especially true when considering host–guest interactions that are non-covalent in nature, and thus exhibit a weaker and less directional binding. A recent advance in this regard involves the use of porous MOFs with high molecular recognition properties which allows guest molecules to become regularly ordered throughout the porous material in such a way to permit the subsequent use of single-crystal X-ray diffraction techniques.[6] This innovative protocol, termed the "crystalline sponge method", has the undeniable advantage of expanding the crystallographic database, by rendering the analysis of liquids and other non-crystallizing compounds possible, however the impact of the host on the structure and electronic properties of the encapsulated guest has not been previously touched upon. Indeed, the confinement effects of the pores may significantly alter the physicochemical properties of the host and/or guest, as demonstrated in a number of zeolites, where the strength of the acidic sites were found to vary.[7] Thus, we investigate for the first time the confinement effects of a crystalline sponge on two organometallic guest compounds.

The host–guest chemistry of MOFs loaded with organometallic species is scarcely reported,[8] however, ferrocene (Fc) appears to be a suitable molecular probe for potential organometallic guest inclusion. While the loading of such guests can be confirmed by spectroscopic methods or by powder X-ray diffraction, an in-depth understanding of the host–guest interactions can only be truly achieved through single-crystal X-ray diffraction. Furthermore, visualization of the host–guest interactions at the atomic level is highly desirable in order to establish conclusive and precise structure–property relationships. Hence, our research efforts were directed towards the inclusion of organometallic sandwich compounds using the crystalline sponge method, which has seen some success in identifying non-trivial guests by single-crystal X-ray diffraction.[9] Furthermore, we also investigate the impact of changing the terminal halide ligand of the host framework from iodide to bromide on the inclusion of the selected guest molecules.

The crystalline sponges were synthesized by the slow diffusion of a solution of zinc iodide or zinc bromide layered onto a solution of tris(4-pyridyl)-1,3,5-triazine (TPT), yielding the doubly interpenetrated porous network $\{[(ZnX_2)_3(TPT)_2]\cdot 5.5(C_6H_5NO_2)\}_n$ (X = I, **1a**; Br, **1b**).[10] These MOFs are ideal hosts for guest inclusion due to their facile synthesis, high stability and presence of large cavities (up to 5 × 8 Å^2). These large voids, or channels, display an inherent affinity for organic molecules, caused by the availability of π···π and charge-transfer interactions of the triazine-based ligand. With this in mind, we decided to first investigate the inclusion of Fc and ferrocene carboxaldehyde (FcCHO), which are highly stable, yet relatively

[a] *Department of Chemistry and Biomolecular Sciences, University of Ottawa, 10 Marie Curie, Ottawa, ON, Canada K1N 6N5. E-mail: m.murugesu@uottawa.ca*
[b] *Institute of Condensed Matter and Nanosciences, MOST – Inorganic Chemistry, Université catholique de Louvain, Place L. Pasteur 1, 1348 Louvain-la-Neuve, Belgium*

† Electronic supplementary information (ESI) available: Synthetic procedures, single-crystal X-ray diffraction data, additional host–guest interaction figures, DRS and PL data. CCDC 1539649–1539651. For ESI and crystallographic data in CIF or other electronic format see DOI: 10.1039/c7cc02470c

small organometallic compounds. Moreover, the encapsulation of a similar family of compounds provides an effective method of directly evaluating the impact of functional groups on the host–guest interactions.

Successful guest encapsulation was evidenced by a remarkable change in colour of the crystals, from nearly colourless to dark-brown. To obtain high quality single-crystals, the mother liquor was carefully decanted, and subsequently replaced by a solution of Fc in an optimal solvent (see the ESI† for details). The single-crystal inclusion of metallocenes in MOFs is non-trivial, as there exists only a handful of examples to date.[11] In the study presented herein, structural refinement reveals the incorporation of Fc in both **1a** and **1b**. In addition to Fc, the pore space of the lattice is completed by partially occupied nitrobenzene and cyclohexane molecules, giving the chemical formulas $\{[(ZnI_2)_3(TPT)_2]\cdot Fc\cdot(PhNO_2)_{0.5}\cdot(C_6H_{12})_2\}_n$ (**2a**) and $\{[(ZnBr_2)_3(TPT)_2]\cdot Fc\cdot(PhNO_2)_{0.46}\cdot(C_6H_{12})_{2.92}\}_n$ (**2b**). Packing arrangements displaying the full contents of the pores can be found in Fig. S1 of the ESI.†

The frameworks of **2a** and **2b** retain the structure of the parent MOFs **1a** and **1b**, respectively, which also leads to a unit cell symmetry that remains in the *C*2/*c* space group (Table S1, ESI†). Following the incorporation of Fc however, we observe a contraction of the *a*-axis, leading to a decrease of the unit cell volume of 3.7 and 8.6% for **2a** and **2b**, respectively (Table S1, ESI†). This contraction provides an initial indication of host–guest interactions, where the flexibility of the interpenetrated structure to accommodate various guest molecules is highlighted. Close inspection of the crystal structures of **2a** and **2b** reveals two Fc molecules in close proximity to one another, with the closest Fe···Fe separations being 6.02 and 5.96 Å, respectively (Fig. 1). It is important to note that an inversion centre resides near the middle of the channels of the MOF, yielding one crystallographically independent Fc molecule for each structure. The cyclopentadienyl (Cp) rings are nearly eclipsed by one another and the average Fe–C distances in Fc were calculated to be 2.03 Å (Tables S2 and S3, ESI†). These structural details and the lack of significant distortions highlight the limited interactions that occur between the Fc guest and the host framework, and are somewhat surprising considering the availability of aromatic rings from the TPT ligand to form face-to-face π···π interactions. Despite such seemingly weak interactions, the Fc guests in **2a** and **2b** are seen to take up the exact same orientation and position within the porous framework. Two conclusions can be drawn here: (i) the terminal halide ligand doesn't appear to have an effect on the positioning of the Fc molecules, and (ii) there is a certain driving force which locks the metallocene guest into this preferred position.

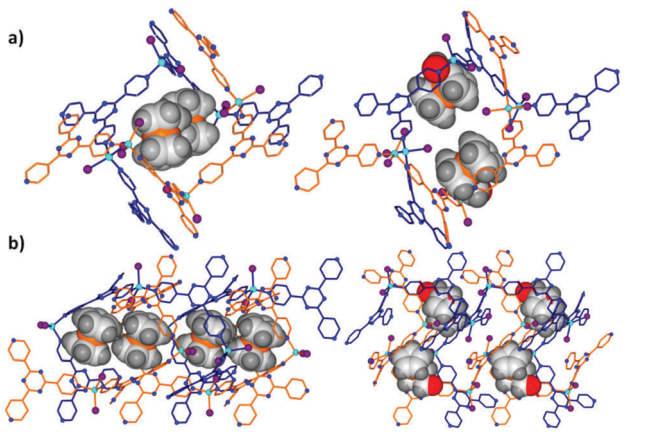

Fig. 1 Molecular structure of the inclusion compounds. (a) Single pore view of **2a** (left) and **3** (right) displaying the orientation and positioning of the Fc-based guests. (b) Side view of the continuous channels highlighting the preferential arrangement of the Fc-based guests in **2a** (left) and **3** (right). Guest molecules are shown using a space-filling model. Solvent molecules, hydrogen atoms of the framework, and positional disorder have been omitted for clarity.

In order to shed some light on this notable behaviour, we have carefully investigated the host–guest interactions (Fig. S2, ESI†). In the case of **2a**, the Fc guest adopts a perpendicular y-shaped arrangement, where the hydrogen and carbon atoms of a Cp ring are seen to interact with two pyridine moieties belonging to the TPT ligand. The electrostatic interactions directing this orientation are the centroid···$HC_{pyridine}$ interactions, which occur at distances of 3.41 and 4.00 Å (Fig. S3a, ESI†). Consequently, these interactions can be described as an intermediate between the T-shaped and edge-to-face π-stacking modes, however, due to the closer interaction of the Cp centroid with one of the H atoms of the pyridine ring, the T-shaped mode is likely more favoured. Contact measurements further revealed C_{Cp}···$HC_{pyridine}$ and $C_{pyridine}H$···HC_{Cp} interactions at distances of 2.74 and 2.39 Å, respectively, the latter of which is slightly smaller than the sum of the van der Waals radii of the individual atoms. On the other side of Fc, the Cp ring also interacts with a pyridine centroid, yielding a slight tilt angle of 2.48° between the planes of the Cp rings. In **2b** however, the Cp rings are very nearly eclipsed and exhibit a slight tilt angle of 0.33° between the two planes. One Cp ring participates in the formation of an H···Br interaction, through a distance of 2.90 Å. The other Cp ring also exhibits a number of π···π interactions between the guest and two framework pyridine rings, as in **2a** (Fig. S3b, ESI†). Interestingly, the same Cp ring also engages in multiple guest–solvent interactions with a cyclohexane molecule, yielding contacts that fall in the range of 2.15–2.88 Å (Fig. S3b, ESI†). Overall, the observed host–guest interactions in **2a** and **2b** are similar, as the relative position of the Fc molecules are identical. Thus, T-shaped π···π interactions play a crucial role in directing the assembly of Fc in **1**, and are prevalent over the face-to-face π···π interactions.

In order to obtain an enhanced understanding of host–guest interactions specific to metallocenes, we have loaded **1a** with FcCHO. The presence of FcCHO in the channels of the MOF was first confirmed by ^{1}H NMR spectroscopy after suitable washings with cyclohexane to remove any surface adsorption. The signals belonging to the framework are not shifted; the two peaks corresponding to the TPT ligand are located at 8.63 and 8.92 ppm, while the four signals corresponding to FcCHO are clearly defined. The single-crystal structure is best refined in the *C*2/*c* space group, and hence, the symmetry of the as-synthesized

MOF remains unchanged. The void space of the MOF is further filled by cyclohexane and benzene solvent molecules, yielding the compound $\{[(ZnI_2)_3(TPT)_2]\cdot(FcCHO)_{2.5}\cdot(C_6H_{12})\cdot(C_6H_6)\}_n$ (**3**), with an asymmetric unit containing two and a half FcCHO molecules. Looking closely at the packing arrangement of **3** (Fig. S4, ESI†), it is evident that the FcCHO guest molecules take up drastically different positions within the pores of the MOF compared to the Fc guests in **2a** and **2b** (Fig. 1). The FcCHO guests are stabilized by a number of interactions with the host framework (Fig. 2). Notably, the guest molecules in **3** participate in face-to-face π···π interactions with the triazine rings of the TPT ligand, as determined by a centroid–centroid distance of 3.40 Å, and a dihedral angle between the mean planes of the guest and host rings of 5.9° (Fig. S5, ESI†). The addition of an –CHO functional group on the guest molecule results in a drastic modification of the host–guest interactions, as was previously observed for a number of small organic benzene-based molecules.[9b] We corroborate that imparting an electron-withdrawing functionality on the guest molecule of interest favors a face-to-face π···π arrangement with either the electron-deficient triazine or pyridyl rings. Hence, we envision being able to control not only the host–guest interactions, but also predict the specific locations of the binding sites through a fundamental understanding of the dominant interactions that drive guest encapsulation.

It is also important to note that the –CHO moieties of all FcCHO guests are positionally disordered over two sites. The preferential arrangement of the guests however, is clearly evidenced by the considerable difference between the occupancies of the –CHO functional group. The orientation which allows the –CHO moiety to interact more closely with the framework is highly favored. The FcCHO guests are further stabilized by multiple π···π interactions with the TPT ligand as well as guest–solvent interactions with benzene.

In order to further investigate the inclusion of the metallocene guests within the pores of the Zn-based MOFs, the pure solid materials were analyzed by diffuse reflectance spectroscopy at room temperature. This allows us to directly probe any confinement effects of the crystalline sponge on the electronic properties of the organometallic guests. Overall, the diffuse reflectance spectra of all guest inclusion compounds exhibit a superposition of the bands observed in the starting MOF and of the selected guests (Fig. S6, ESI†). This is not entirely surprising since all guest molecules only exhibit non-covalent interactions with the host framework. The non-covalent interactions are, however, of different nature and strength, as evidenced by the single-crystal X-ray structures. The latter may be used to explain the significantly higher intensity of the shoulder at 600–800 nm in the spectra of **2a** and **2b**, when compared to the intensity of the same shoulder in the spectrum of Fc, which is negligible. Conversely, the shoulders in the visible range of **3**, which account for the presence of FcCHO, are lower in intensity when compared to the spectrum of pure FcCHO. Consequently, the interaction of the metallocene guests with the crystalline sponge **1**, most likely influences the d–d transitions, and hence, the HOMO–LUMO energy gap of the encapsulated guests.

To complement the diffuse reflectance spectroscopy experiments, the solid-state photoluminescence properties of **1a**, **2a** and **3** were also investigated. The data were collected using an excitation wavelength of 300 nm, giving an excitation profile in the 350–550 nm region (Fig. S7, ESI†). Thus, we report for the first time the fluorescent behaviour of the parent crystalline sponge **1a**, which exhibits weak blue emission with a broad maximum at 442 nm. The inclusion of Fc and FcCHO effectively quenches the photoluminescence of the framework. As shown in a few other cases,[8b,11b] the excitation energy is transferred to the Fc, and is then quenched following an energy transfer mechanism.

To further probe guest confinement effects, we turned our attention to solid-state nuclear magnetic resonance spectroscopy (SSNMR). More specifically, ^{13}C CPMAS SSNMR allows us to directly measure rotation of the Cp rings, and provides us with information on how compartmentalization of Fc in **1** may affect the dynamic motion of the guest. Spectra were collected using the dipolar dephasing technique, which involves allowing a short delay without high power proton decoupling between the cross polarization contact time and the beginning of the FID data collection.[12] With this method, and under these conditions, all rigid proton bearing carbon signals (–CH– and $–CH_2–$) will typically dephase to zero intensity during a 40 μs dephasing delay because of the strong $^{13}C–^{1}H$ dipolar coupling. Non-proton bearing carbon signals, such as those from quaternary or carbonyl carbons, have reduced $^{13}C–^{1}H$ dipolar coupling due to the longer distance between the carbon and the proximate protons. As a result, their signals will dephase to a much lesser extent and survive the dephasing delay with attenuation based on the degree of dipolar coupling to the protons. The same is true for the signals of highly mobile proton bearing carbon signals such as those from rotating methyl groups. In this case, the $^{13}C–^{1}H$ dipolar coupling is reduced as a result of molecular motion, and, like the non-protonated carbons, their signals will survive the dephasing delay with attenuation based on the degree of dipolar coupling to

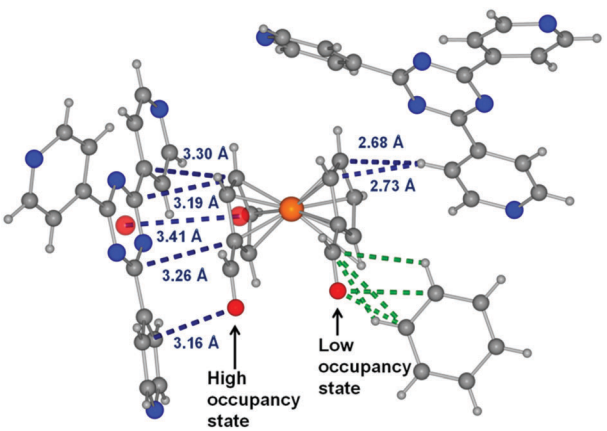

Fig. 2 Stabilization of the FcCHO guests in **3**, through numerous close contacts. Host–guest interactions are shown in dashed blue bonds, while guest–solvent interactions are in green. Ring centroids are displayed as transparent red spheres. Positional disorder of the FcCHO molecule, with high and low occupancy states, is shown to highlight the full range of host–guest interactions.

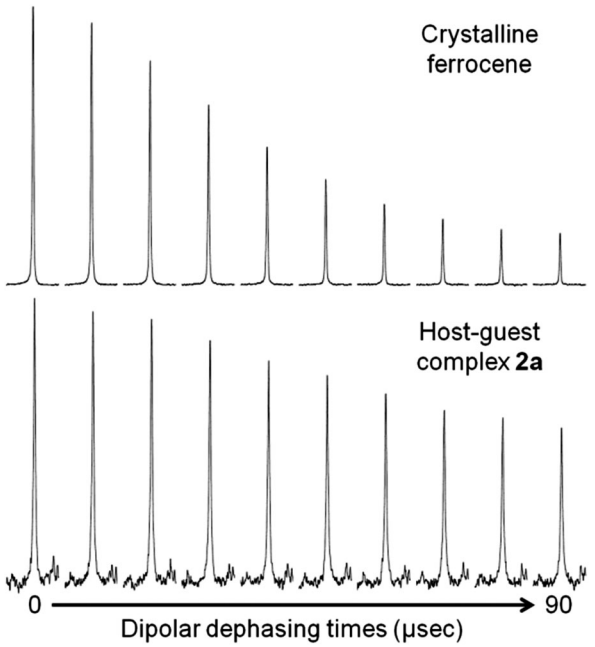

Fig. 3 Comparison of the ^{13}C CP MAS SSNMR signals from the Cp rings of crystalline Fc and **2a** with dipolar dephasing times from 0–90 μs.

the protons. The ^{13}C signal from the Cp rings of a pure crystalline Fc sample and the guest Fc in **2a** is shown in Fig. 3 as a function of the dipolar dephasing delay. It is clear that in both cases the Cp signal survives dephasing delays much longer than 40 μs, indicating that the Cp rings are mobile. It is also apparent that the attenuation of the Cp signals in **2a** is much less than that for pure Fc at all dephasing delays, which is indicative that the guest Fc in **2a** is much more mobile than pure Fc. Previous reports on pure Fc have established that the Cp rings are in fact already capable of rotating freely.[13] Thus, these data suggest that the barrier for rotation of the Cp ring is drastically altered once confined within **1a**. The surprising enhancement of the mobility of the Cp rings may be explained by a sterically less hindered environment, compared to crystalline Fc, in which the molecules are packed in a tight and efficient manner. Indeed, the structure of Fc exhibits a packing arrangement in which the Cp rings adopt a perpendicular y-shaped geometry.[14] The representative π···π interactions are compared to that of **2a** and **2b**, and yield much closer contacts (Table S2, ESI†). These results clearly illustrate how the confinement of guest molecules in select environments, *i.e.* a network of weak non-covalent interactions, can impact molecular motion.

In summary, we have successfully encapsulated metallocenes within a crystalline sponge and evaluated the host–guest interactions through single-crystal X-ray diffraction. Notably, we demonstrated that T-shaped π···π interactions are pivotal in the orientation of the Fc molecules, while face-to-face π···π interactions become predominant upon addition of an electron-withdrawing group on the Cp ring. We have also probed the confinement effects of the benchmark crystalline sponge, through diffuse reflectance spectroscopy, photoluminescence and SSNMR. Remarkably, the confinement effects of a crystalline sponge have resulted in a significant disparity in the internal ring rotation of the Cp rings between samples of pure Fc and of Fc encapsulated within a nanoporous framework. Through this confinement effect study, we have highlighted how the crystalline sponge method, which offers a decisive power in the structural determination of guest molecules, can drastically impact the structure and electronic properties of guest molecules.

We thank the University of Ottawa, NSERC (Discovery, RTI and PGS-D grants) and CFI for their financial support. Dr C. D. McTiernan and Prof. J. C. Scaiano are also kindly acknowledged for assistance with the luminescence measurements.

Notes and references

1 J.-R. Li, J. Sculley and H.-C. Zhou, *Chem. Rev.*, 2012, **112**, 869–932.
2 J. Lee, O. K. Farha, J. Roberts, K. A. Scheidt, S. T. Nguyen and J. T. Hupp, *Chem. Soc. Rev.*, 2009, **38**, 1450–1459.
3 J. D. Rocca, D. Liu and W. Lin, *Acc. Chem. Res.*, 2011, **44**, 957–968.
4 N. A. Khan, Z. Hasan and S. H. Jhung, *J. Hazard. Mater.*, 2013, **244**, 444–456.
5 (*a*) T. K. Maji, G. Mostafa, R. Matsuda and S. Kitagawa, *J. Am. Chem. Soc.*, 2005, **127**, 17152–17153; (*b*) C.-L. Chen and A. M. Beatty, *J. Am. Chem. Soc.*, 2008, **130**, 17222–17223; (*c*) M. J. Manos, E. J. Kyprianidou, G. S. Papaefstathiou and A. J. Tasiopoulos, *Inorg. Chem.*, 2012, **51**, 6308–6314.
6 Y. Inokuma, S. Yoshioka, J. Ariyoshi, T. Arai, Y. Hitora, K. Takada, S. Matsunaga, K. Rissanen and M. Fujita, *Nature*, 2013, **495**, 461–466.
7 (*a*) E. G. Derouane and C. D. Chang, *Microporous Mesoporous Mater.*, 2000, **35–36**, 425–433; (*b*) G. Sastre and A. Corma, *J. Mol. Catal. A: Chem.*, 2009, **305**, 3–7.
8 (*a*) M. Meilikhov, K. Yusenko and R. A. Fischer, *Dalton Trans.*, 2010, **39**, 10990–10999; (*b*) P. P. Mazzeo, L. Maini, D. Braga, G. Valenti, F. Paolucci, M. Marcaccio, A. Barbieri and B. Ventura, *Eur. J. Inorg. Chem.*, 2013, 4459–4465; (*c*) R. Heck, O. Shekhah, O. Zybaylo, P. G. Weidler, F. Friedrich, R. Maul, W. Wenzel and C. Wöll, *Polymers*, 2011, **3**, 1565–1574.
9 (*a*) X.-F. Gu, Y. Zhao, K. Li, M.-X. Su, F. Yan, B. Li, Y.-X. Du and B. Di, *J. Chromatogr. A*, 2016, **1474**, 130–137; (*b*) L. M. Hayes, C. E. Knapp, K. Y. Nathoo, N. J. Press, D. A. Tocher and C. J. Carmalt, *Cryst. Growth Des.*, 2016, **16**, 3465–3472; (*c*) T. R. Ramadhar, S.-L. Zheng, Y.-S. Chen and J. Clardy, *Chem. Commun.*, 2015, **51**, 11252–11255; (*d*) L. M. Hayes, N. J. Press, D. A. Tocher and C. J. Carmalt, *Cryst. Growth Des.*, 2016, **17**, 858–863; (*e*) G. Brunet, D. A. Safin, M. Z. Aghaji, K. Robeyns, I. Korobkov, T. K. Woo and M. Murugesu, *Chem. Sci.*, 2017, **8**, 3171–3177.
10 K. Biradha and M. Fujita, *Angew. Chem., Int. Ed.*, 2002, **41**, 3392–3395.
11 (*a*) H. Kim, H. Chun, G.-H. Kim, H.-S. Lee and K. Kim, *Chem. Commun.*, 2006, 2759–2761; (*b*) S. A. Sapchenko, D. G. Samsonenko, D. N. Dybtsev, M. S. Melgunov and V. P. Fedin, *Dalton Trans.*, 2011, **40**, 2196–2203.
12 S. J. Opella and M. H. Frey, *J. Am. Chem. Soc.*, 1979, **101**, 5854–5856.
13 (*a*) A. Haaland and J. E. Nilsson, *Acta Chem. Scand.*, 1968, **22**, 2653–2670; (*b*) A. Gardner, J. Howard, T. Waddington, R. Richardson and J. Tomkinson, *Chem. Phys.*, 1981, **57**, 453–460.
14 F. Takusgawa and T. F. Koetzle, *Acta Crystallogr., Sect. B: Struct. Crystallogr. Cryst. Chem.*, 1979, **35**, 1074–1081.

